



This is a repository copy of *Effect of CaO/Al<sub>2</sub>O<sub>3</sub> ratio on physical properties of lime-alumina-based mould powders*.

White Rose Research Online URL for this paper:

<https://eprints.whiterose.ac.uk/199041/>

Version: Published Version

---

**Article:**

Seyrek, M. [orcid.org/0000-0001-5386-4804](https://orcid.org/0000-0001-5386-4804) and Thackray, R. [orcid.org/0000-0003-2573-0221](https://orcid.org/0000-0003-2573-0221) (2023) Effect of CaO/Al<sub>2</sub>O<sub>3</sub> ratio on physical properties of lime-alumina-based mould powders. *Metals*, 13 (4). 719. ISSN 2075-4701

<https://doi.org/10.3390/met13040719>

---

**Reuse**

This article is distributed under the terms of the Creative Commons Attribution (CC BY) licence. This licence allows you to distribute, remix, tweak, and build upon the work, even commercially, as long as you credit the authors for the original work. More information and the full terms of the licence here:

<https://creativecommons.org/licenses/>

**Takedown**

If you consider content in White Rose Research Online to be in breach of UK law, please notify us by emailing [eprints@whiterose.ac.uk](mailto:eprints@whiterose.ac.uk) including the URL of the record and the reason for the withdrawal request.



[eprints@whiterose.ac.uk](mailto:eprints@whiterose.ac.uk)  
<https://eprints.whiterose.ac.uk/>

## Article

# Effect of CaO/Al<sub>2</sub>O<sub>3</sub> Ratio on Physical Properties of Lime-Alumina-Based Mould Powders

Mustafa Seyrek <sup>1</sup>  and Richard Thackray <sup>2,\*</sup> <sup>1</sup> Vocational School of Technical Sciences, Hitit University, Çorum 19169, Turkey<sup>2</sup> Department of Materials Science and Engineering, The University of Sheffield, Sheffield S1 3JD, UK

\* Correspondence: r.thackray@sheffield.ac.uk

**Abstract:** High-aluminium steels contain a significant amount of aluminium. The reaction between Al in the liquid steel and SiO<sub>2</sub> in lime-silica-based mould powders during the continuous casting process of high Al steel causes chemical compositional changes in the mould powders, subsequently affecting the surface quality of slabs. In order to solve the aforementioned problem, lime-alumina-based mould powders have been developed, which can lead to an increase in the surface quality of cast slabs by inhibiting steel/slag interaction. However, the mould slag tends to crystallise easily, which leads to a deterioration of the mould lubrication. In view of this aspect, it is important to develop and optimize lime-alumina-based mould powders to meet the requirements of continuous casting of high-aluminium steels. In this study, the changes in crystallinity, viscosity and melting temperature of lime-alumina-based mould powders with the effects of increasing the CaO/Al<sub>2</sub>O<sub>3</sub> ratio have been observed through STA (Simultaneous Thermal Analysis), HSM (Hot Stage Microscopy), XRD (X-ray Diffraction), IPT (Inclined Plate Test) and rotational viscometer. The crystallisation behaviour of these mould powders was evaluated by generating CCT (continuous cooling transformation) diagrams. Additionally, the changes in steel chemistry have also been analysed using XRF (X-ray fluorescence) and ICP (Inductively Coupled Plasma Mass Spectrometer). The results of these analyses demonstrated that crystallinity of lime-alumina-based mould powder is increased while the initial crystallisation temperature and viscosity are decreased by CaO/Al<sub>2</sub>O<sub>3</sub> additions. However, the degree of steel/slag interaction decreases with an increase in Al<sub>2</sub>O<sub>3</sub> content.



**Citation:** Seyrek, M.; Thackray, R. Effect of CaO/Al<sub>2</sub>O<sub>3</sub> Ratio on Physical Properties of Lime-Alumina-Based Mould Powders. *Metals* **2023**, *13*, 719. <https://doi.org/10.3390/met13040719>

Academic Editors: Noé Cheung and John Campbell

Received: 4 January 2023

Revised: 31 March 2023

Accepted: 1 April 2023

Published: 6 April 2023



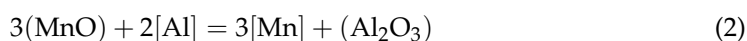
**Copyright:** © 2023 by the authors. Licensee MDPI, Basel, Switzerland. This article is an open access article distributed under the terms and conditions of the Creative Commons Attribution (CC BY) license (<https://creativecommons.org/licenses/by/4.0/>).

**Keywords:** high-Al steels; mould powder; C/A ratio; crystallinity; steel-slag interaction

## 1. Introduction

Due to their high strength/weight ratio and excellent formability, advanced high strength steels for automotive applications have garnered a lot of attention in recent years. Aluminium contents in these steels varies from 0.5 wt.% to 3 wt.%. Aluminium is not only a very frequently used type of nonferrous metal but also a unique chemical element for alloying and is used in the de-oxidation of liquid steel during the steel making process. Aluminium is also known as a grain refiner for improved toughness, as a certain amount of Al addition to steels results in fine grains [1].

Throughout the past decades, high-Al steels have been manufactured by the continuous casting process. It has been stated that, during continuous casting, the high amount of dissolved aluminium in the steel is apt to react with less stable oxides, as shown below in the SiO<sub>2</sub>-based mould powder.



These reactions decrease the mould powder performance and cause operational problems, such as the sticking of mould powder to the water-cooled copper mould and the

increase in cracking owing to lubrication difficulty. Research has been conducted to find a solution by optimising SiO<sub>2</sub>-based mould powders. However, it is difficult to optimise lime-silica-based mould powders for high-Al steels based upon the reactions that occur between the liquid slag and steel [1,2].

In recent times, CaO-Al<sub>2</sub>O<sub>3</sub>-based mould powders have been developed for casting of high-Al steels. In these newly developed mould powders, SiO<sub>2</sub> is partly replaced by Al<sub>2</sub>O<sub>3</sub> in order to prevent the reactions at the slag/steel interface. As a result, it has been stated that the slag/steel interaction is prevented and operational problems are significantly decreased when using these new powders. However, the mould slag in these powders tends to crystallise easily and it can lead to variations in mould slag lubrication and heat transfer, which in turn causes a deterioration of the casting process and a decrease in the slab surface quality [3–5]. Blazek et al. [6] revised the CaO-Al<sub>2</sub>O<sub>3</sub>-SiO<sub>2</sub> phase diagram and pointed out that the lowest melting temperature is with a CaO/Al<sub>2</sub>O<sub>3</sub> ratio of 1 at ~10 wt.% SiO<sub>2</sub>. This work illustrated that the lowest melting temperatures for CaO-Al<sub>2</sub>O<sub>3</sub> and CaO-SiO<sub>2</sub> compositions are comparable and indicate that the same amount of fluidisers would be favourable.

In order to improve the crystallisation behaviour of CaO-Al<sub>2</sub>O<sub>3</sub>-based mould powders, intensive effort has been made. Jiang et al. [7] revealed that the addition of alumina tends to enhance the crystallinity and critical cooling rate, as the crystallisation temperature increases with an increase of the CaO/Al<sub>2</sub>O<sub>3</sub> ratio ranging from 0.8 to 1.2 in lime-alumina-based mould powders. Fu et al. [5] studied the effect of the lime/alumina ratio on crystallisation and the results showed that the thickness of the slag film varies according to the lime/alumina ratio. Zhao et al. [2] found that MnO could enhance the general heat transfer by promoting melting and preventing the crystallisation of the mould powder. Boxun et al. [8] pointed out that Li<sub>2</sub>O and Na<sub>2</sub>O in lime-alumina mould powders prevent crystallisation of the mould powder by decreasing the initial crystallisation temperature and increasing incubation time. Cheng et al. [3] stated that the crystallisation temperature of CaO-Al<sub>2</sub>O<sub>3</sub>-based mould powders decreased with the addition of B<sub>2</sub>O<sub>3</sub>. Finally, Huang et al. [1] reported that the viscosity and break temperature of mould powders decrease with an increase in B<sub>2</sub>O<sub>3</sub> content.

During the various studies that have been carried out, the viscosity, crystallisation and melting behaviour of CaO-Al<sub>2</sub>O<sub>3</sub>-based mould powders, over a range of ratios, were not systematically investigated. Therefore, it is important to study the regulation of CaO-Al<sub>2</sub>O<sub>3</sub> mould powder for casting of high-Al steels.

A general approach for the development of lime-alumina-based mould powders is that the CaO/Al<sub>2</sub>O<sub>3</sub> ratio (C/A ratio) has a significant effect on slag crystallisation. Hence, it is important to determine the optimal C/A ratio by investigating the effects of compositional change on slag properties. There are a few studies [5,7,9] which have investigated the effects of the C/A ratio on thermo-physical properties of lime-alumina-based mould powders. These studies mainly focus on crystallisation of the mould powder with small changes in C/A ratio. Therefore, it is required to investigate the effect of a wide range of C/A ratios on thermo-physical properties of lime-alumina-based mould powders.

In a previous study, the authors [10] investigated the effect of the CaO/Al<sub>2</sub>O<sub>3</sub> ratio on the viscosity of lime-alumina-based mould powders using various methods, including the Inclined Plate Test, FactSage software, and empirical models (Riboud and Urbain). They found that increasing the CaO/Al<sub>2</sub>O<sub>3</sub> ratio resulted in a sudden decrease in viscosity, followed by a gradual stabilization. In this paper, the authors built upon this previous work by examining additional key properties of mould powders with an increased CaO/Al<sub>2</sub>O<sub>3</sub> ratio, including changes in crystallinity, steel chemistry via steel/mould powder interaction tests and melting temperature. Furthermore, they employed a rotational viscometer to investigate the viscosity of the designed mould powder in further detail.

It is important that newly developed mould powders have low surface cracking, optimum consumption rate and chemical stability during casting. The purpose of this article is

to provide a concise summary of the findings from a series of laboratory tests conducted on lime-alumina-based mould powders for use in the casting of high aluminium steels.

## 2. Materials and Methods

### 2.1. Materials

In this study, five different types of mould powder were produced to analyse the effect of the C/A ratio on thermo-physical properties of lime-alumina-based mould powder. Mould powders were produced from pure chemical reagents CaO, Al<sub>2</sub>O<sub>3</sub>, SiO<sub>2</sub>, B<sub>2</sub>O<sub>3</sub> (the purity of all chemicals was >99%), along with Na<sub>2</sub>CO<sub>3</sub> and Li<sub>2</sub>CO<sub>3</sub> as the source of Na<sub>2</sub>O and Li<sub>2</sub>O. Their chemical compositions were chosen considering a variation in the C/A ratio and are given in Table 1. These lime-alumina-based mould powders included five compositions where the C/A ratio ranges from 1 to 3. Constant amounts of Li<sub>2</sub>O (5 wt.%), Na<sub>2</sub>O (10 wt.%) and B<sub>2</sub>O<sub>3</sub> (15 wt.%) were used in all samples to provide a multicomponent effect.

**Table 1.** Chemical composition of C-series mould powders used in this study (in wt.%).

Powder	C/A	SiO <sub>2</sub>	CaO	Al <sub>2</sub> O <sub>3</sub>	Li <sub>2</sub> O	Na <sub>2</sub> O	B <sub>2</sub> O <sub>3</sub>
C1	1	10	30	30	5	10	15
C2	1.5	10	36	24	5	10	15
C3	2	10	40	20	5	10	15
C4	2.5	10	43	17	5	10	15
C5	3	10	45	15	5	10	15

### 2.2. Methods for Measuring Crystallinity

Due to the possibility of having carbon in the raw powders, all mould powders were decarburised at 650 °C for 16 h in air. The samples were prepared by melting 30 g of raw powders in a platinum crucible. The mould powders were melted at 1500 °C in an induction furnace for 20 min to eliminate bubbles and homogenise their chemical composition. After that, the slag was poured into a stainless-steel crucible, which was in an ice-water bath. The glassy discs obtained were dried and cut in half, with one half used for metallographic determination and the other half for X-ray Diffraction.

The glassy discs, after melting, were sectioned using a diamond blade and mounted by a cold mounting technique in 40 mm diameter cups. Then, the samples were ground and polished using 1 µm solution before etching. Etching was done with HF acid at a concentration of 2.5% for 2 s. The samples were then observed with an optical microscope and the % crystallinity of samples was calculated by revealing the crystalline and glassy parts in the samples. Olympus Stream (Evident Corporation, Tokyo, Japan) image analysis software was used to be able to determine the amount of glassy and crystalline fractions of the samples.

The other halves of the solidified samples after melting were crushed and ground with a mortar and pestle and then sieved using a 300-mesh screen for use in the X-ray Diffractometer. A Bruker D2 Phaser (Bruker, Billerica, MA, USA) was employed for XRD analysis and the results were analysed using the Diffrac.Suite (Bruker AXS GmbH, Karlsruhe, Germany) software package. The X-ray diffraction data were collected in a range of  $2\theta = 10$  to 80 deg with a rate of 10 deg/min using CuK<sub>α</sub> radiation (1.54184 Å).

The crystallinity in the mould powder samples was calculated from its XRD scan. As it can be seen in Figure 1, XRD patterns of a glassy phase do not give peaks but give a ‘bump’. The percentage of the amorphous phase can be calculated with the help of the area under this bump and the area under the peaks [11].

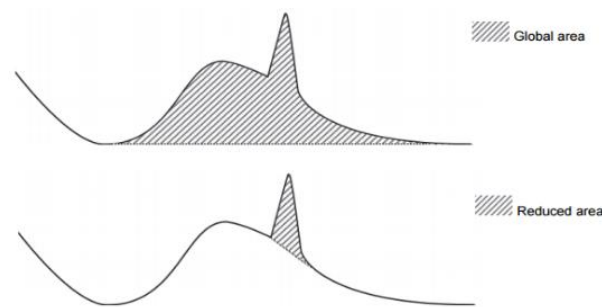


**Figure 1.** Global and reduced area under an XRD scan.

The formula used to calculate the percentage of amorphous phase and % of crystallinity is as follows [12]:

$$\% \text{Amorphous} = \frac{\text{Global area} - \text{Reduced area}}{\text{Global area}} \times 100 \quad (3)$$

$$\% \text{Crystallinity} = 100 - \% \text{Amorphous} \quad (4)$$

### 2.3. Methods for Examination of Melting and Crystallisation Behaviour

A Misura 3.32 Heating Microscope (TA Instruments, New Castle, DE, USA) was employed to determine the melting temperature of the mould powder. The raw powders were dampened with distilled water to be able to shape a sample which was cohesive enough for compactness. The powders were shaped into a 3 mm high and 2 mm diameter cylindrical mould with the help of a pressing tool and were placed on a small alumina plate. Then, this alumina plate was moved into the tube furnace with the help of two rods. Figure 2 illustrates the schematic of the heating microscope.

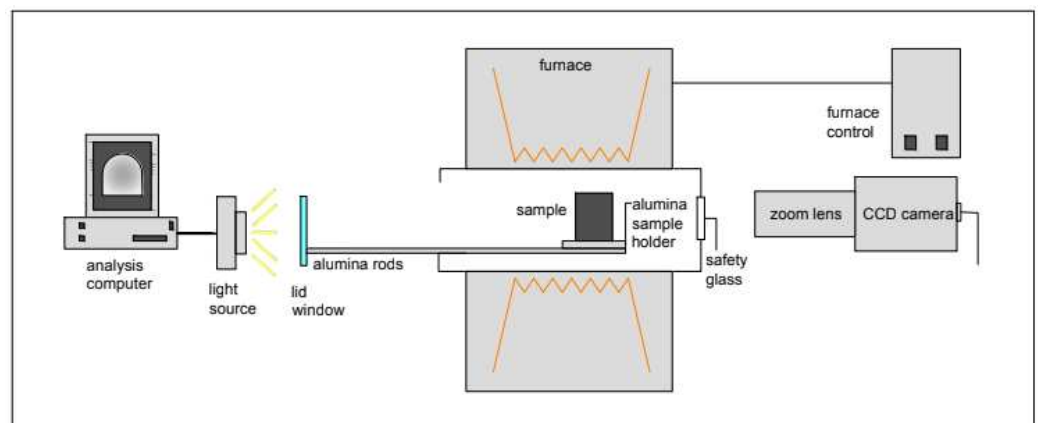


**Figure 2.** Schematic of Misura Heating Microscope used in this study.

First, the sample was heated at a rate of 50 °C/min to 900 °C and then heated at a rate of 6 °C/min until it was completely melted in air. The rate of heating and the changes in the sample shape were automatically recorded by image analyser software during the heating. The melting temperature of each powder sample was detected by the software once the height of the sample was reduced to 15% of its original height.

In this study, a TA Instruments Q600 SDT (TA Instruments, New Castle, DE, USA) was employed to examine the crystallisation behaviour and determine the glass transition temperatures of the mould powders. First, 30 mg samples were placed in a platinum crucible and heated from room temperature to 1500 °C at a heating rate of 10 °C/min in an argon atmosphere. Samples were held for 60 s at 1500 °C to homogenise the slag chemical composition and eliminate the bubbles. Subsequently, the slag was cooled to room temperature at different cooling rates of 5 °C/min, 10 °C/min, 15 °C/min and 20 °C/min.

CCT (Continuous Cooling Transformation) diagrams were constructed by recording the relationship between time and temperature. Thermal profiles of the CCT experiments can be seen in Figure 3.

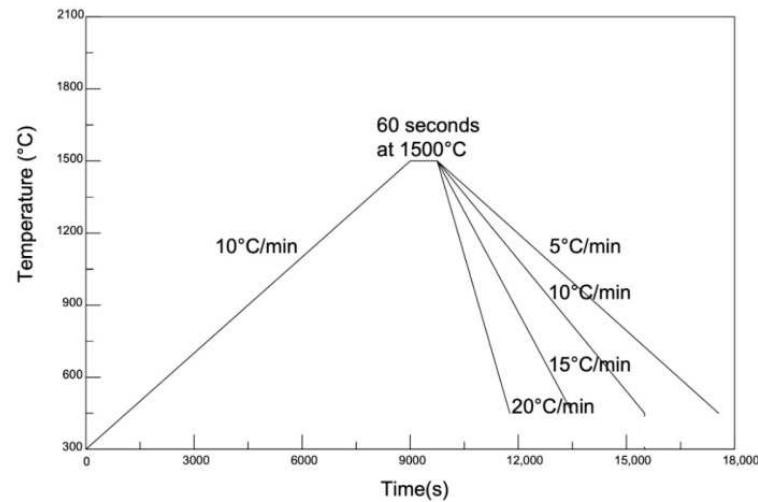


**Figure 3.** Thermal profile of CCT experiments.

#### 2.4. Methods for Measuring Viscosity

To be able to select the most convenient mould powder for continuous casting, knowledge of various mould powder physiochemical properties, such as viscosity and break temperatures, is required. In this study, the rotating viscometer method and the Inclined Plane Test (IPT), which are detailed below, were applied to measure the viscosity of the mould powders.

##### 2.4.1. Inclined Plane Test (IPT)

The inclined plane test is a simple method, which is used to measure the viscosity of mould powders at 1300 °C. A V-shaped stainless-steel plate is arranged at 14° inclinations with the help of a supporting block. The experimental set-up can be seen in Figure 4.

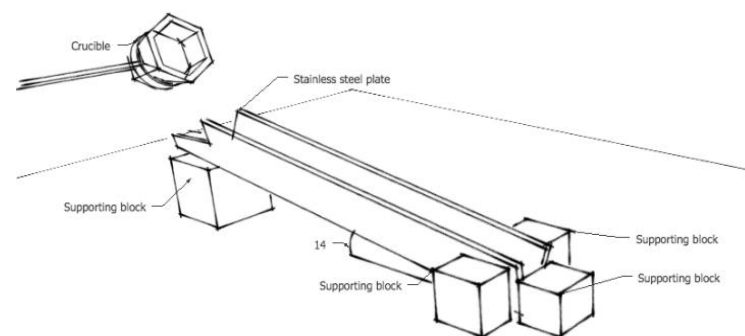


**Figure 4.** The experimental set-up of the inclined plane test.

The mould powders were decarburised at 700 °C for 12 h. First, 15 g of the decarburised mould powder was placed in a graphite crucible and held in a muffle furnace at 1300 °C. After 10 min, the crucible was removed from the furnace and the slag was directly poured over the top of the inclined plane. The slag flows down the inclined plane until it loses its fluidity. It forms as a ribbon on the inclined plane and the viscosity of the mould powder at 1300 °C was calculated from the length of the slag ribbon.

The relationship between powder viscosity and ribbon length is as follows:

$$\eta = C_1 \exp\left(\frac{C_2}{L_R}\right) \quad (5)$$

where  $\eta$  is viscosity of mould powder in  $\text{dPa}\cdot\text{s}$ ,  $L_R$  is the length of the ribbon and  $C_1$  and  $C_2$  are constants, which are determined as 0.2656 and 470, respectively [13].

#### 2.4.2. Rotational Viscometry

High temperature viscosity measurements for C1, C3 and C5 mould powders were carried out with a Bahr VIS 403 HF (BAHR Thermoanalyse GmbH, Hullhorst, Germany) rotational viscometer. The experimental set-up of the rotating bob viscometer is shown in Figure 5. For this test, the mould powders were decarburised at  $650\text{ }^\circ\text{C}$  for 12 h. The decarburised powders were melted at  $1300\text{ }^\circ\text{C}$  for 10 min and then the slag was quenched onto a steel plate. The samples were broken into small pieces and 24 g of the sample was placed into the viscometer in a Pt crucible. The crucible was heated up to  $1400\text{ }^\circ\text{C}$  and the rotating bob immersed into the slag. The temperature was lowered at  $10\text{ }^\circ\text{C}/\text{min}$  and data were collected simultaneously by the software until it reached the maximum torque of 49 mNm.

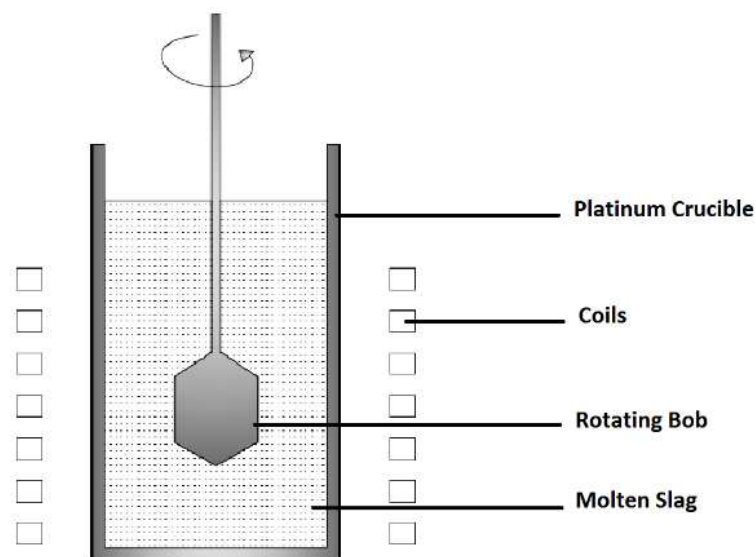


**Figure 5.** Schematic diagram of the experimental set-up for the rotational viscometer test.

#### 2.4.3. FactSage

FactSage (Thermfact/CRCT, Montreal, QC, Canada and GTT-Technologies, Aachen, Germany) software was used to calculate the viscosity of the designed mould powders at  $1100\text{ }^\circ\text{C}$ ,  $1200\text{ }^\circ\text{C}$ ,  $1300\text{ }^\circ\text{C}$  and  $1400\text{ }^\circ\text{C}$  from the chemical composition of the mould powders. For FactSage calculations, the database for melts was selected because this is valid for supercooled and liquid slags. This database generally corresponds to temperatures above  $900\text{ }^\circ\text{C}$ . Data entry for lithium oxide on FactSage is not available. Therefore, the lithium oxide content of the mould powder was added to sodium oxide for the viscosity calculations.

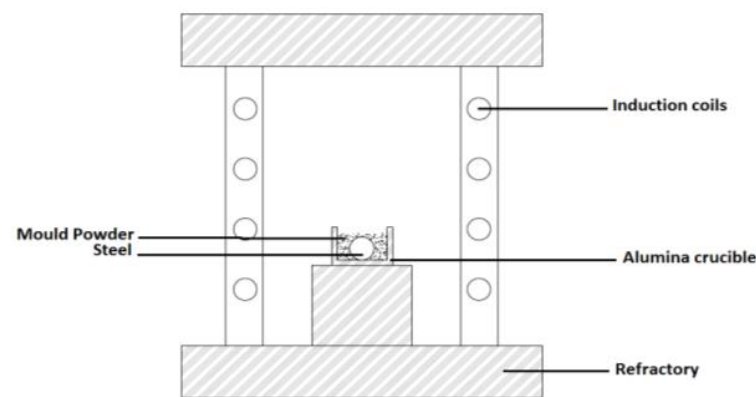
#### 2.5. Examination of Steel-Slag Interaction

This part of study was aimed at investigating the mass transfer between the steel and slag. Table 2 shows the chemical composition of the high-aluminium TRIP steel which was used in this test.

**Table 2.** Chemical composition of high-Al TRIP steel obtained from X-ray fluorescence.

Composition (wt.%)	Fe	Mn	Al	Si	Gd
Steel	96.672	1.345	0.954	0.667	0.287

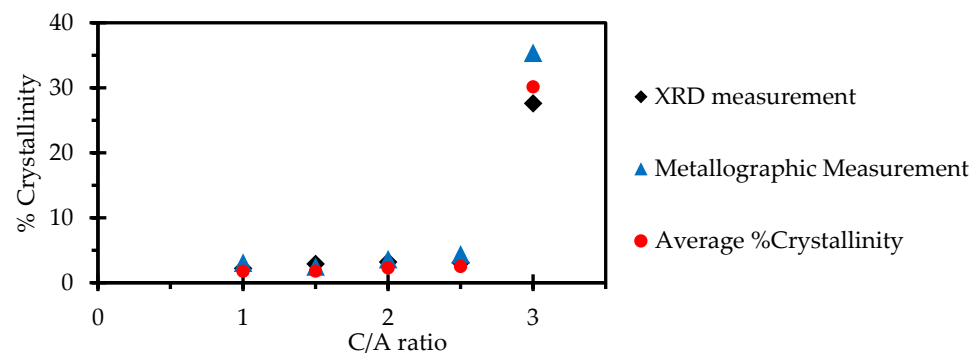
For this study, an alumina crucible (99.8% purity) with 20 mm height and 19 mm diameter was employed. First, the TRIP steel was cut into small pieces and approximately 3 g of steel was added into the alumina crucible and then the rest of the crucible was filled with mould powder (~5 g); this alumina crucible was then placed into the furnace. The crucible was kept in the furnace at 1500 °C for 20 min in air and then taken out from the furnace and cooled. A schematic diagram of the steel-slag test is shown in Figure 6. Crucibles were then cut into half by a diamond blade on a SECOTOM-50 and mounted by the cold mounting technique into 40 mm cups. The steel samples were removed from the alumina crucible after the steel-slag interaction tests and analysed in an ICP (Inductively Coupled Plasma Mass Spectrometer) instrument after first dissolving them in HF acid.

**Figure 6.** Schematic of steel–slag interaction test setup.

### 3. Results and Discussion

#### 3.1. Effect of $\text{CaO}/\text{Al}_2\text{O}_3$ Ratio on the Crystallinity of Mould Powder

The crystallinity of C-series mould powders was investigated by X-ray Diffraction and metallographic determination techniques. The results obtained with these tests are given in Figure 7. Cross sectional images of each C-series mould powders are illustrated in Figure 8. The XRD patterns of the C-series lime-alumina-based mould powders are presented in Figure 9. The crystallinity of C-series mould powders gradually increased by increasing the  $\text{CaO}/\text{Al}_2\text{O}_3$  ratio from 1 to 2.5, while a sudden increase in crystallization was observed when the ratio was increased from 2.5 to 3.

**Figure 7.** The percent crystallinity in C-series mould powders as a function of C/A ratio.



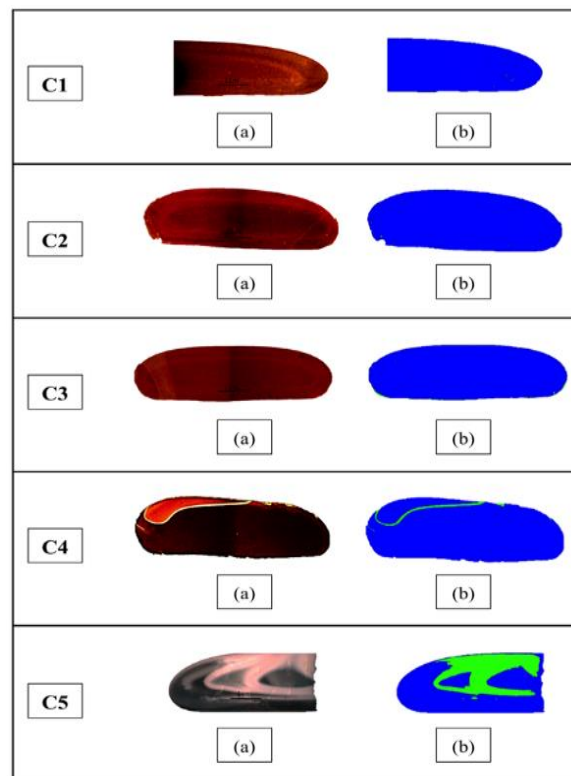


**Figure 8.** (a) Cross sectional images of C-series mould powders. (b) Threshold analysis of C-series mould powder (crystal parts in green and glassy parts in blue).

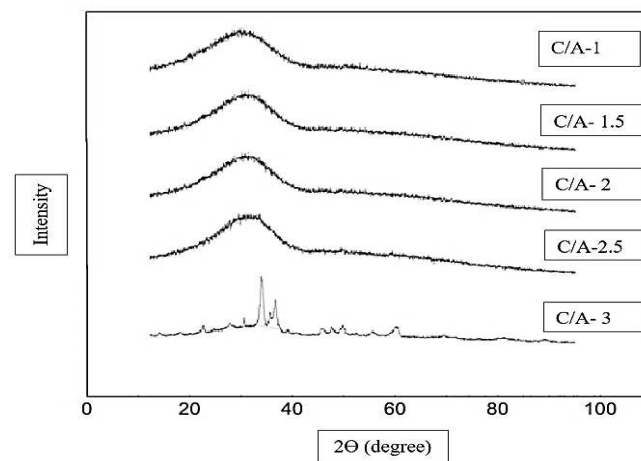


**Figure 9.** The XRD patterns of C-series mould powders with different C/A ratio.

The amount of crystalline phase obtained by X-ray Diffraction for the mould powder samples is compared with the values obtained using metallographic measurements in Figure 7. As can be seen from this figure, the crystallinity measured by both techniques for C-series mould powders present the same trend. However, the crystallinity obtained by metallographic measurement for C5 (C/A = 3) is higher than the crystallinity measured by X-ray Diffraction even though the crystallinity results obtained by both techniques for the rest of the four samples are in good agreement.

As illustrated in Figure 7, crystallisation of the mould powders increases with an increase in the C/A ratio ranging from 1 to 3. The  $\text{Al}_2\text{O}_3$  content of the mould powder ranged from 15 wt.% to 30 wt.% in the C-series mould powders.  $\text{Al}_2\text{O}_3$  works as an acidic oxide with an increase in  $\text{Al}_2\text{O}_3$  which turns slag into an alumina-silicate structure, which is a more complicated structure and inhibits crystallisation. Crystallinity of the mould

powders with C/A ratios of 1, 1.5, 2 and 2.5 are relatively low. Low crystallinity in these samples may be associated with the B<sub>2</sub>O<sub>3</sub>, Li<sub>2</sub>O and Na<sub>2</sub>O content of these powders. C-series mould powders contain a constant 15 wt.% of B<sub>2</sub>O<sub>3</sub> and boron trioxide is generally accepted as a very strong glass former which weakens the crystallinity tendency of the mould powder [14,15].

The C-series mould powders also contain a constant amount of Li<sub>2</sub>O and Na<sub>2</sub>O. The current observations indicate that the appropriate amount of Li<sub>2</sub>O and Na<sub>2</sub>O addition restrains the crystallinity of lime-alumina-based mould powders [3,16,17]. Lu et al. [8] systematically investigated the effect of Li<sub>2</sub>O and Na<sub>2</sub>O addition on the crystallinity of lime-alumina-based mould powder. The results indicate that the increase of Li<sub>2</sub>O and Na<sub>2</sub>O restrains the crystallisation of lime-alumina-based mould powder by increasing the incubation time for crystalline growth and decreasing the initial crystallisation temperature.

The increase in the C/A ratio ranged from 1 to 2.5 and resulted in a small increase in the crystallinity of samples. The interesting phenomenon is that an increase in the C/A ratio to 3 caused a large increase in the crystallinity. This increase in crystallinity may be explained by the CaO addition since it increases the basicity of mould powder which is represented by %CaO/%SiO<sub>2</sub>. It has been indicated that basicity has been used to measure the degree of depolymerisation of the melt and an increase in basicity could promote the crystallisation of mould powder [18]. Li, Thackray and Mills [19] suggest that the number of non-bridging oxygen per tetrahedrally coordinated atom as represented by the NBO/T ratio is associated with the crystallinity of the mould powder and is calculated as follows:

$$\frac{NBO}{T} = \frac{2X_{CaO} + 2X_{BaO} + 2X_{CaF2} + 2X_{Na2O} - 2X_{Al2O3} + 6X_{Fe2O3} + (2X_{MgO} + 2X_{MnO})}{X_{SiO2} + 2X_{Al2O3} + X_{TiO2} + 2X_{B2O3} + (X_{MgO} + X_{MnO})} \quad (6)$$

They noted also that the critical point arises at the NBO/T ratio of 2. Above this critical point, the crystallinity of the mould powder increases linearly with increasing the NBO/T ratio, while below the critical point mould powders have very low crystallinity. As can be seen in Table 3, C5 (C/A = 3) is only powder, which exceeds that critical point. As the NBO/T ratios of powders C1, C2, C3 and C4 (see Table 3) are below 2, they are designated as glassy. The main reason for this difference between X-ray Diffraction measurement and metallographic measurement could be the appearance of transition zones (glass + crystalline) in the C5 mould powder. As the crystallinity is relatively high for C5 (C/A = 3), transition zones appear on the cross-section image of the sample and that is the main source of uncertainty because the image analysis software could not separate phases perfectly during the thresholding. The other reason for the uncertainties associated with the metallographic determination technique could be the size of the area viewed. As the technique uses a small area of the sample to measure the crystallinity, local inhomogeneities could cause variations in the crystallisation of the sample. Therefore, the viewed area of the sample may not represent the whole sample.

**Table 3.** NBO/T ratio of C-series mould powder used in this study.

Powder	C1	C2	C3	C4	C5
NBO/T ratio	0.9	1.3	1.7	1.9	2.2

In this study, XRD patterns of C-series mould powders have been used to calculate % crystallinity of powders by using the area under the peaks or bumps. Figure 7 shows the crystallinity of C-series mould powders obtained by X-ray Diffraction with a varying CaO/Al<sub>2</sub>O<sub>3</sub> ratio. As can be seen in Figure 9, apart from the powder with a C/A of 3, the other powders present bumps on their XRD scans, indicating that they are almost completely glassy.

### 3.2. Effects of CaO/Al<sub>2</sub>O<sub>3</sub> Ratio on the Crystallisation Behaviour of the Mould Flux

The crystallisation behaviour of the C-series lime-alumina-based mould powders were also investigated by employing STA (Simultaneous Thermal Analysis) at various cooling rates. The crystallisation temperatures of slags combined with recorded time-temperature data were used to construct CCT diagrams of mould powders for the cooling rates of 5, 10, 15 and 20 °C/min, as shown in Figure 10.

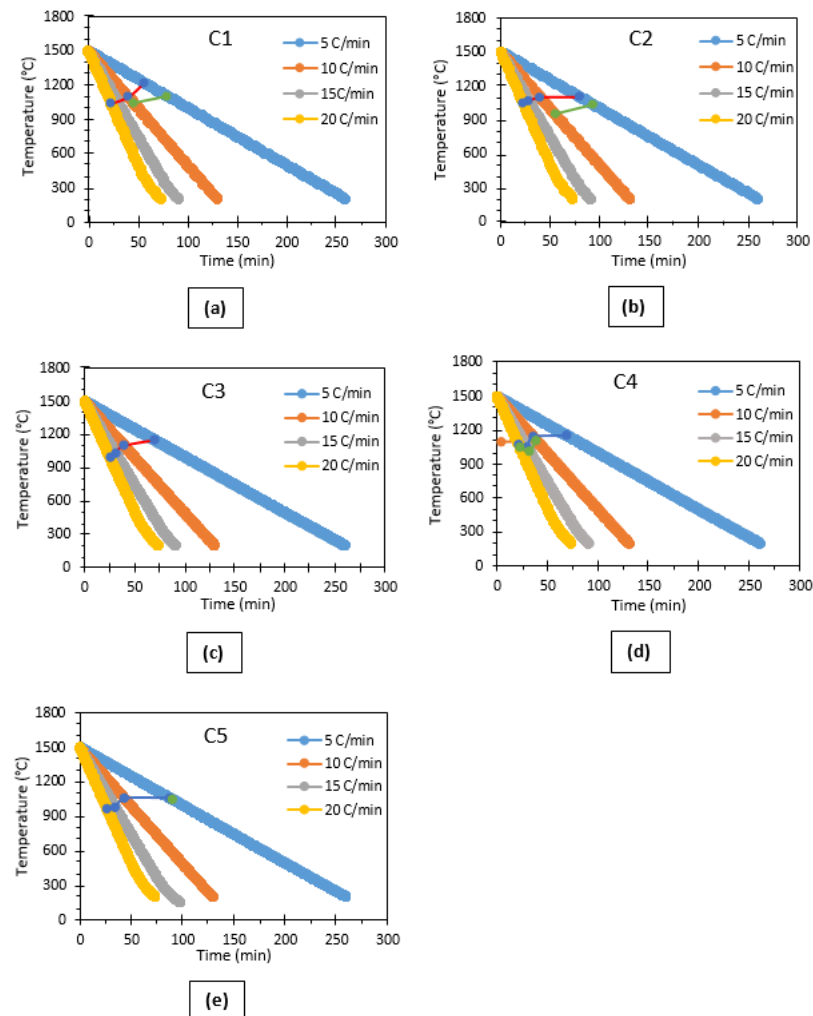


**Figure 10.** CCT diagrams of mould powders with different C/A ratios: (a) C/A = 1, (b) C/A = 1.5, (c) C/A = 2, (d) C/A = 2.5, (e) C/A = 3.

The results demonstrate that the crystallisation temperature of crystalline phases in C-series mould slags decreased with an increasing cooling rate in the STA measurements. A likely explanation is that an increase in the continuous cooling rate will increase the viscosity of the mould powder by increasing the degree of undercooling. Due to the increase in diffusion resistance, it requires a greater driving force for the nucleation and growth of crystals in slag. Therefore, the crystallisation temperature decreases to supply the requirements for a larger driving force.

It can be observed from Figure 10 that there are two exothermic peaks in the C1 and C2 curves at the 5 and 10 °C/min cooling rates, which prove the presence of two successive crystallisation events. Only the C3 mould powder presented a single crystallisation event at all cooling rates. On the other hand, mould powder C1 does not present a crystallisation event at the cooling rate of 15 °C/min, and C1 (the lowest C/A ratio) presents the highest crystallisation temperature at 1216 °C at the cooling rate of 5 °C/min among all the mould powders.

Figure 11 represents the relationship between the C/A ratio and the initial crystallisation temperatures of C-series mould powders at a cooling rate of 15 °C/min. The results indicate that the initial crystallisation temperature decreases from 1190 °C to 979 °C with an increase of the C/A ratio from 1 to 3. This indicates that an increase in the C/A ratio inhibits the tendency for crystallisation. When the C/A ratio was higher than 1.5, the decreasing effect became weaker.

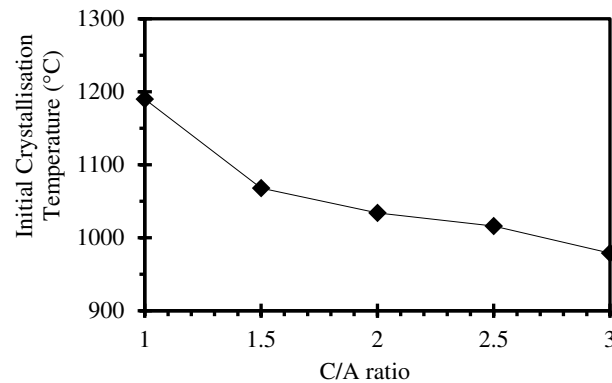


**Figure 11.** Effect of ratio on initial crystallisation temperature at a cooling rate of 15 °C/min.

The results obtained in this part of the study are in agreement with the results of Jiang et al. [7]. They systematically studied the effect of the C/A ratio on the crystallisation of lime-alumina-based slag systems by employing single and double hot thermocouple technology and suggested that initial crystallisation temperature decreased with an increasing C/A ratio. It can be found that the % crystallinity results do not present the same trend with results obtained from continuous cooling during the STA measurements. While not conclusive, the differences between these two trends could be for the following reasons:

- i. Cooling rates in STA measurements are lower than those in the % crystallinity measurements.
- ii. The higher amount of mould powder used in the % crystallisation tests could increase the natural convection which is beneficial for crystallisation.

Various parameters have been reported regarding the thermal stability in glasses [20]. Turnbull [21] revealed a parameter based on the nucleation theory and used the  $T_g/T_m$  ratio as a criterion for glass formation ( $K_T$ ), where  $T_g$  is glass transition temperature and  $T_m$  is melting temperature.

$$K_T = T_{rg} = \frac{T_g}{T_m} \quad (7)$$

Mills and Dacker [22] defined the liquidus temperature ( $T_{liq}$ ) as the temperature where the casting powder becomes completely molten. They used the following equation to calculate the liquidus temperature and  $T_{liq}$  values have been used of  $T_m$  values in this part of the study.

$$T_{liq} (^{\circ}\text{C}) = 1200 - 1.518\%\text{SiO}_2 + 2.59\%\text{CaO} + 1.56\%\text{Al}_2\text{O}_3 - 17.1\%\text{MgO} - 9.06\%\text{Na}_2\text{O} - \%\text{K}_2\text{O} + \%\text{Li}_2\text{O} + 4.8\%\text{F} - 9.87\%\text{FeO} - 2.12\%\text{MnO} \quad (8)$$

Turnbull [21] also used the term of reduced glass transition temperature ( $T_{rg}$ ) as the avoidance of a single nucleation event and indicated that it is equal to  $K_T$ . Zanotto and Coutinho [23] proposed that a high value of  $T_{rg}$  would result in high viscosity and eventually lead to a low critical cooling rate. They also suggest that a  $T_{rg}$  lower than 0.58–0.60 would lead to homogeneous nucleation while a  $T_{rg}$  greater than 0.58–0.60 would lead to heterogeneous crystallisation. According to the  $K_T$  values listed in Table 4, C-series mould powders display homogeneous crystallisation as the  $K_T$  values are lower than 0.58–0.60. Sharda et al. [24] also pointed out that  $T_{rg}$  indicates ease of glass formation. In this sense, the value of  $T_{rg}$  for all powders remains nearly constant, which indicates the good glass forming ability of these samples.

**Table 4.** Temperature in °C of  $T_g$ ,  $T_{liq}$  and  $T_x$  and values of  $K_T$  and  $K_H$  determined by using above equations.

Samples	$T_g$ (°C)	$T_{liq}$ (°C)	$T_x$ (°C)	$K_T$	$K_H$	$T_x - T_g$
C1	700.2	1218	1190	0.57	17.5	498.8
C2	694.6	1223	1068	0.57	2.4	373.4
C3	691.1	1229	1034	0.56	1.8	342.9
C4	688.6	1232	1016	0.56	1.5	327.4
C5	686.9	1234	979	0.56	1.1	292.1

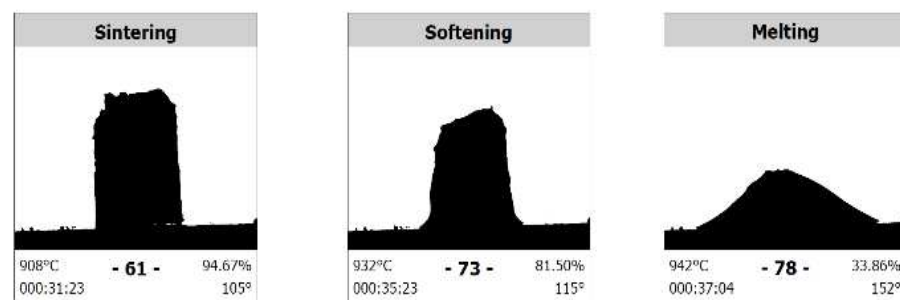
Inoue et al. [25,26] revealed another parameter for glass forming ability, which is temperature difference between  $T_x$  and  $T_g$ . They also mentioned that higher value in this difference ( $T_x - T_g$ ) means more delay in the nucleation process.  $T_x$  is the initial crystallisation temperature here. Hruby [27] also proposed a glass forming ability parameter as  $K_H$ , which is also used as a measure of glass forming tendency. The formula for the Hruby parameter is given below and  $K_H$  values for C-series mould powder are listed in Table 4.

$$K_H = \frac{T_x - T_g}{T_m - T_x} \quad (9)$$

According to calculated values for  $K_H$ , C1 has the highest glass forming tendency among the C-series mould powders. This is consistent with data obtained by % crystallinity method as C5 has the highest crystallisation tendency among the C-series mould powders. In terms of C1, C2, C3 and C4,  $K_H$  values increase with the decrease of the C/A ratio ranging from 1 to 2.5. That means that the glass forming tendency decreases with an increase in the C/A ratio.  $Al_2O_3$  content of mould powder ranged from 15 wt.% to 30 wt.% in C-series mould powder.  $Al_2O_3$  works as an acidic oxide with an increase in  $Al_2O_3$ , which turns slag into an alumina-silicate structure, which is a more complicated structure and promotes glass formation.

### 3.3. Effect of CaO/ $Al_2O_3$ Ratio on Melting Behaviour

Hot Stage Microscopy was employed to study the effect of C/A on melting behaviour of lime-alumina-based mould powders. The camera was used to take a picture of the sample every 2 °C and representative pictures for sintering, softening and melting temperatures of the C1 powder are illustrated in Figure 12.

**Figure 12.** Sample pictures taken by the Hot Stage Microscopy camera for sintering, softening and melting temperatures of C1 powder.

As can be observed in Figure 13, when the C/A ratio increased from 1 to 2.5, the recorded melting temperature of the samples slightly increased in the initial stage, then stabilised at about 960 °C and finally there was a dramatic increase in the melting temperature when the C/A ratio increased from 2.5 to 3.

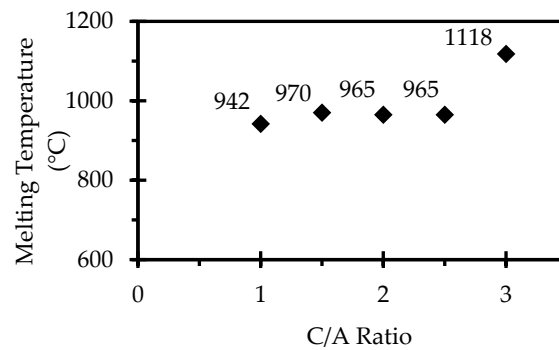


**Figure 13.** Effect of C/A ratio on the melting temperature of C-series mould powders.

It should be noted that the results obtained in this part of the study are not in agreement with the general consideration that an increase of  $\text{Al}_2\text{O}_3$  content results in an increase of melting temperature. Blazek et al. [6] systematically investigated the effect of the C/A ratio on lime-alumina-based mould powders for casting high-aluminium TRIP steels and suggested that melting temperature decreased when the C/A ratio ranged from 0.6 to 3.6. Similarly, Yu et al. [28] investigated the effect of  $\text{Al}_2\text{O}_3/\text{SiO}_2$  on the melting temperature of mould powders and suggested that melting points increase with increased  $\text{Al}_2\text{O}_3$  addition.

Only one study, which was published in 2017 by Qi, Liu and Jiang [29], is available and that indirectly agrees with this study. The authors concluded that melting temperatures of powders nearly stabilised at around  $1140\text{ }^\circ\text{C}$  when the C/A ratio ranged from 1 to 1.82. A probable explanation was raised from the authors' work that with increasing the C/A ratio, mould powder components, such as  $\text{Al}_2\text{O}_3$ , CaO and  $\text{SiO}_2$ , can form as compounds of lower melting temperature, which may decrease the melting temperature of the melt. Conversely,  $\text{LiO}_2$  and  $\text{Al}_2\text{O}_3$  tend to react to be able to form phases with high melting temperature with an increase in the C/A ratio. These two opposite effects present nearly the same influence, and hence the melting temperature of mould powders present a stabilised trend when the C/A ratio increases from 1 to 2.5. The mould powders in this study contain a constant amount of  $\text{LiO}_2$ ,  $\text{Na}_2\text{O}$  and  $\text{B}_2\text{O}_3$ .

### 3.4. Effect of $\text{CaO}/\text{Al}_2\text{O}_3$ Ratio on Viscosity

In this part of the study, three different techniques were used to obtain the viscosity of the C-series mould powders at different temperatures. First, the IPT (Inclined Plane test) was utilised. During the test, the relationship between ribbon length of the powders and viscosity was determined. Figure 14 illustrates the change in viscosity as a function of the C/A ratio at  $1300\text{ }^\circ\text{C}$ . As can be clearly seen in Figure 14, the viscosity decreases dramatically when the C/A ratio changes from 1 to 1.5. With the increase in the C/A ratio from 1.5 to 2.5, the viscosity slightly decreases, then when the C/A ratio is greater than 2.5, the viscosity starts to level off.

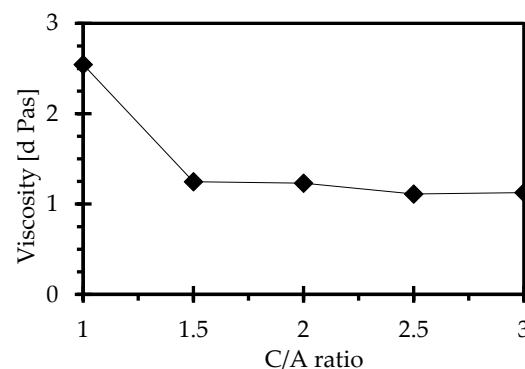


**Figure 14.** Effect of C/A ratio on viscosity measured by the IPT method.

Secondly, the viscosity of the mould powders was measured by the rotating bob viscometer. Figure 15 shows the viscosity–temperature curves of the C1, C2 and C3 mould powders. It can be observed that increasing temperature results in a decrease in each powder viscosity. Viscosity decreases with an increase in the C/A ratio in the temperature range from 1090 °C to 1300 °C. However, at temperatures below 1088 °C, the viscosity of samples increases rapidly with decreasing temperature.

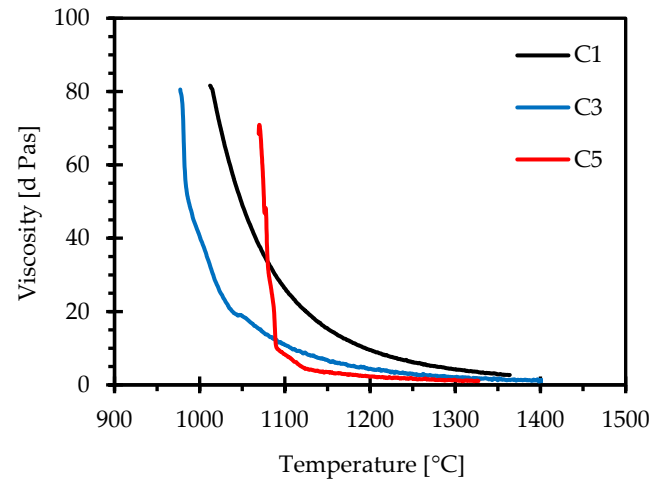


**Figure 15.** Viscosity–temperature curves of C1, C2 and C3 samples obtained from the rotating bob viscometer.

Thirdly, the FactSage software was employed to verify the reproducibility of the viscosity measurements obtained by the IPT and Rotating Bob Viscometer. Since the IPT test was only able to measure the viscosities of the C series mould powders at 1300 °C, and the rotating bob viscometer was used only to measure the viscosity of the C1, C2 and C3 samples, the viscosities of all the C series samples between 1300–1500 °C were estimated using FactSage software. The effect of temperature on the viscosity of C-series mould powders at different C/A ratios is plotted in Figure 16, where it can be seen that viscosity decreases with increasing temperature at all C/A ratios as expected. The viscosity of all the powders rapidly decreases when the temperature increases from 1300 °C to 1400 °C and the viscosity only gradually decreases when the temperature increases from 1400 °C to 1500 °C. However, at the temperatures of 1300 °C, 1400 °C and 1500 °C, the viscosity the mould powders decrease with an increase in the C/A ratio.

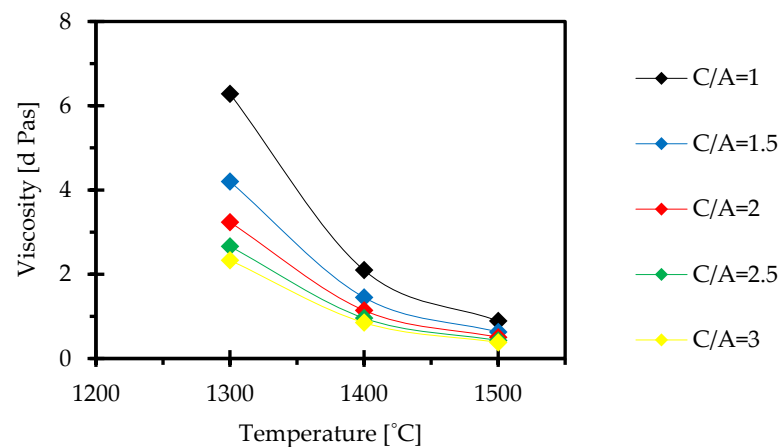


**Figure 16.** Viscosity of C-series mould powders estimated by FactSage software as a function of temperature.

Figure 17 illustrates the comparison of experimental data obtained by IPT and rotating bob viscometer with the viscosities estimated by FactSage. As it can be noted from Figure 17, the viscosity of mould powders obtained by these methods presents the same trend and both measured and estimated viscosities decrease with an increase in C/A ratio. Viscosity measurement methods used in this study were credible when the experimental uncertainties associated with viscosity determination tests were considered. However, a good correlation between the measured and the calculated viscosities was observed.

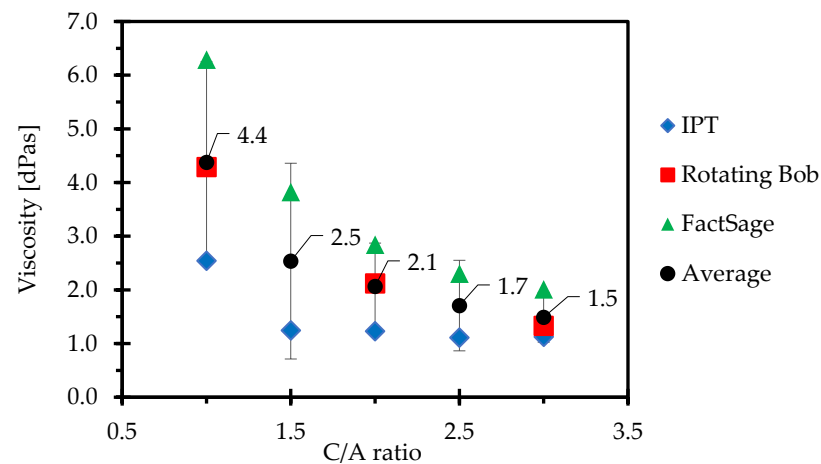


**Figure 17.** Comparison of measured and estimated viscosity of C-series mould powders at 1300 °C.

It is known that  $\text{Al}_2\text{O}_3$  is an amphoteric oxide and has a remarkable effect on the viscosity of mould powder. It behaves as a basic oxide (network modifier) or an acidic oxide (network former) depending on the basicity of the slag. The nature of alumina in the melt is detailed in the literature extensively. In lime-alumina melts, Al-O complexes present 4-, 5- and 6-fold coordination and form as  $\text{AlO}_4$ ,  $\text{AlO}_5$  and  $\text{AlO}_6$  units [30–32]. At higher temperatures, more alumina is involved in the formation of aluminate structures with a decrease in C/A ratio. This increases the degree of polymerization and causes an increase in the viscosity of melt. On the other hand, with an increase in C/A ratio, more  $\text{O}^{2-}$  ions are free to depolymerise the aluminate network, and hence reduce the viscosity of the melt [9,18,33,34]. At lower temperatures, particles with higher melting temperatures start to precipitate in the melt and solid particles begin controlling the viscosity, and therefore the viscosity of the mould powder increases.

For the powders used in this part of the study, the mole fraction of basic oxides (CaO and  $\text{Na}_2\text{O}$ ) is much greater than the mole fraction of  $\text{Al}_2\text{O}_3$ . Therefore, alumina behaves as an acidic oxide to be able to promote  $[\text{AlO}_4]^{5-}$  ions when adequate charge balance is available by favour of basic oxides. Any excess  $\text{Ca}^{2+}$  cations in the CaO- $\text{Al}_2\text{O}_3$  melt depolymerise the  $\text{AlO}_4$  structural units and decrease the viscosity. Therefore, in our C-series mould powders, viscosity decreases with an increase in the C/A ratio. As can be seen in Figure 14, the viscosity sharply decreases and then gradually becomes stable with an increase in the C/A ratio. This is due to the fact that a further increase in the C/A ratio supplied an excess of free  $\text{O}^{2-}$  ions, and thus viscosity ultimately becomes stable.

The results obtained from this part of the study are consistent with the reported results. Yan et al. [9] systematically studied the effect of the C/A ratio on the viscosity behaviour of lime-alumina-based mould powders by utilising the rotational cylinder method and concluded that at temperatures above 1270 °C, the viscosity first dramatically decreased and then gradually became stable. They also confirmed this behaviour with the aid of Fourier Transform Infrared (FTIR) spectra. Kim and Sohn [34] also revealed that the viscosity is lowered with an increase in the C/A ratio from 0.8 to 1.2. The C-series mould powders used in this study contain 5% $\text{Li}_2\text{O}$  and 15% $\text{B}_2\text{O}_3$ .  $\text{Li}^+$  is very active when it has very low electrostatic potential to merge with  $\text{O}^{2-}$ . Therefore, it offers free  $\text{O}^{2-}$  ions in the melt and presents basic behaviour in the mould powder which destroys the structure in the melt



and decreases viscosity [28].  $B_2O_3$  is an acidic oxide and considered as a network former in melts. Therefore, the addition of  $B_2O_3$  increases the acidity of mould and lowers the viscosity [18,29,35].

### 3.5. Effect of $CaO/Al_2O_3$ Ratio on the Steel-Slag Interaction

In order to investigate the mass exchange at the steel/slag interface, lab-scale experiments were carried out for each C-series mould powder at a temperature of 1500 °C. Figure 18 shows the amount of [Al] changes in steel as a function of the C/A ratio of the mould powders. As can be observed in Figure 18, the [Al] content in steel decreases with an increase in the C/A ratio. The change in total manganese content of steel at each C/A ratio can be seen in Figure 19. It is known that the most significant chemical reaction, which takes place at the steel/slag interface, is the reduction of  $SiO_2$  by the dissolved Al in steel [36]. The C-series lime-alumina-based mould powders used here contain a constant amount of 10 wt.%  $SiO_2$  and this  $SiO_2$  is reduced by Al in the steel through the following reaction:

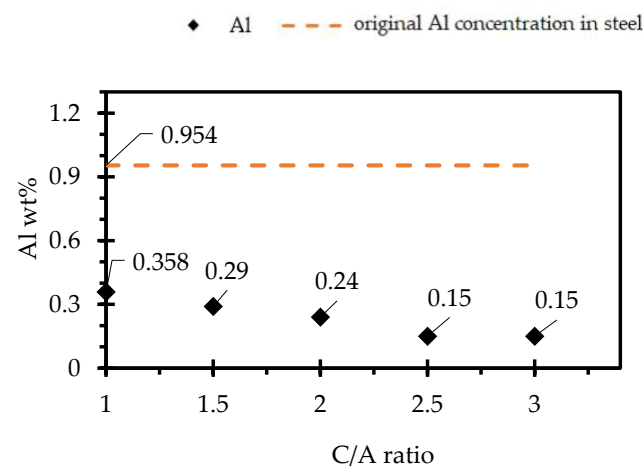
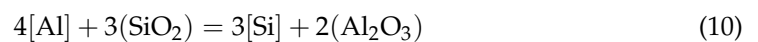


**Figure 18.** Change in total aluminium content of steel depending on C/A ratio for the 20 min interaction time.

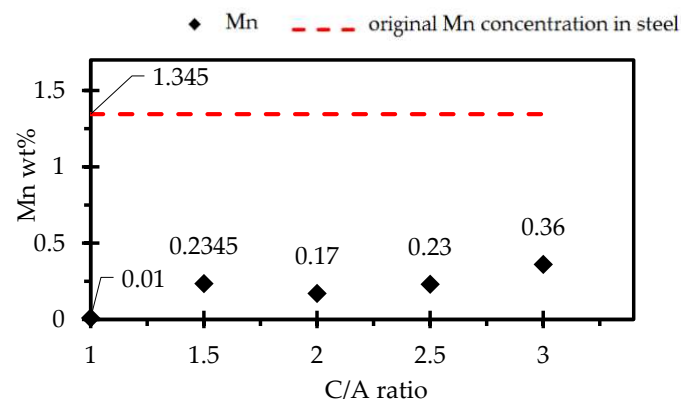


**Figure 19.** Total change in the manganese content of the steel depending on the C/A ratio for the 20 min interaction time.

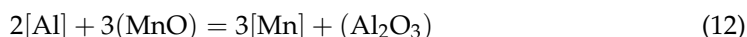
According to Figure 18, the reactivity between slag and steel increases with an increase in the C/A ratio. This phenomenon can be related to the  $Al_2O_3$  content in C-series mould powders. The higher amount of  $Al_2O_3$  may suppress the reaction of the  $SiO_2$  reduction as the  $Al_2O_3$  content of the mould powder increases with a decrease in C/A ratio. Therefore,

the decrease in the total amount of [Al] in steel increases with an increase in the C/A ratio for these mould powders.

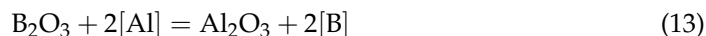
On the other hand, there is one study which disagrees with the above conclusion. Kim et al. [37] evaluated the compositional change between molten high-Al steel and lime-silica-based mould powder and suggested that the initial Al<sub>2</sub>O<sub>3</sub> content in mould powder does not have an effect on SiO<sub>2</sub> reduction. As the steel sample contains a high amount of [Mn], the following reaction may occur between SiO<sub>2</sub> in slag and Mn in steel.



It is interesting to note that no [Mn] was detected by XRF in the steel, which was in contact with the powder with a C/A ratio of 1. However, as shown in Figure 19, the effect of the C/A ratio on the total change of manganese content in the steel is not clear. The reason for this uncertainty could be due to the following reaction where the high [Al] content in steel reduced the oxidised MnO content again.



In summary, both total [Al] and [Mn] contents in steel have decreased after steel/slag interaction. This means that the C/A ratio does not affect the degree of steel/slag interaction and the SiO<sub>2</sub> content in these C-series mould powders is not low enough to prevent reactions between steel and slag. On the other hand, these C-series mould powders contain B<sub>2</sub>O<sub>3</sub> and as an acidic oxide, B<sub>2</sub>O<sub>3</sub> has a similar effect on slags to that of SiO<sub>2</sub> and may react with the high dissolved [Al] in steel through the following reaction:



where the reduced B may go into the steel. (C-series mould powders contain 15% B<sub>2</sub>O<sub>3</sub>). As XRF does not detect boron, further investigation was carried out by Inductively Coupled Plasma (ICP) mass spectrometry to see the effect of B<sub>2</sub>O<sub>3</sub> content on the steel/slag interaction.

The ICP test results confirm that the original steel sample does not have boron present. Figure 20 shows how the amount of [B] changes in steel as a function of the C/A ratio of the mould powders. As can be observed in Figure 20, the steel picked up a small amount of B. It is pointed out by Kim et al. [37] that the Na<sub>2</sub>O content of the mould powder may be reduced by [Al] in steel in the case of insufficient SiO<sub>2</sub> in the mould powder as:

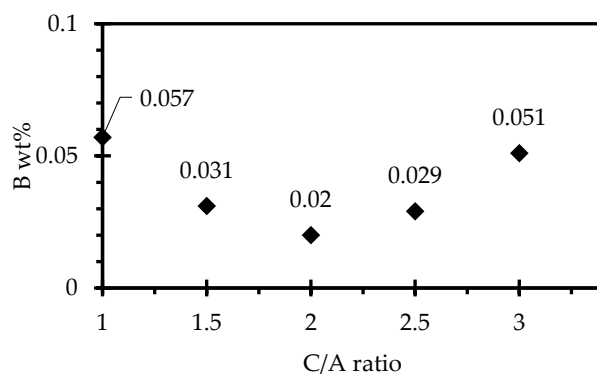
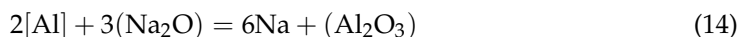


**Figure 20.** Total change in the boron content of the steel depending on the C/A ratio for the 20 min interaction time.

#### 4. Conclusions

In this study, the changes in crystallinity, viscosity and melting temperature of lime-alumina-based mould powder with the effect of increasing the CaO/Al<sub>2</sub>O<sub>3</sub> ratio have been observed through STA (Simultaneous Thermal Analysis), HSM (Hot Stage Microscopy), XRD (X-ray Diffraction), IPT (Inclined Plate Test) and rotational viscometer, which may provide guidelines for the design of lime-alumina-based mould powders for the continuous casting of high-Al steels. The crystallisation behaviour of these mould powders was evaluated by generating CCT (continuous cooling transformation) diagrams. The changes in steel chemistry have also been analysed using XRF (X-ray fluorescence) and ICP. Additionally, FactSage software was used to calculate the viscosity of the mould powders.

1. According to the X-ray Diffraction results, the powder with a C/A ratio of 3 has relatively high crystallinity in comparison with the other C-series mould powders, which was also confirmed by metallographic determination measurements. In addition, CCT test results indicate that an increase in C/A ratio decreases the initial crystallisation temperature of these mould powders at a cooling rate of 15 °C/min. This demonstrates that the percentage of crystallinity of C-series mould powders as obtained by X-ray Diffraction are not in accordance with the CCT test results.
2. The results of the HSM tests indicated that the melting temperature of lime-alumina-based mould powders increased when the C/A ratio ranged from 1 to 3. However, these results are not consistent with the literature data for conventional mould powders.
3. Viscosity measurements with the IPT technique show that the viscosity sharply decreases and then gradually stabilises with an increase in the C/A ratio. The rotating bob viscometer analysis of C1, C3 and C5 mould powders showed that the results were in line with the above findings, which lends to the credibility of this study. A good correlation between the measured and the calculated viscosities was observed for these mould powders.
4. The results from the steel/slag interaction tests show that the degree of steel/slag interaction decreases with an increase in Al<sub>2</sub>O<sub>3</sub> content.

From this study, lime-alumina-based mould powders with a C/A ratio in the range 1.5–2 have a low degree of steel/slag interaction, a low melting temperature and viscosity. Therefore, these conditions may significantly improve the lubrication effects of these mould powders during casting and consequently enhance the heat transfer by reducing the crystallisation tendency. Although further studies are required to understand more about the effects of composition on mould powder performance, the work done here to study the effect of the C/A ratio, indicates that improved lubrication properties and suppressed crystallinity mean that mould powders with a C/A ratio in this range may be suitable candidates for use in the casting of high Al steels.

**Author Contributions:** Writing—original draft, M.S.; Writing—review & editing, R.T.; Supervision, R.T. All authors have read and agreed to the published version of the manuscript.

**Funding:** This research received no external funding.

**Institutional Review Board Statement:** Not applicable.

**Informed Consent Statement:** Not applicable.

**Data Availability Statement:** The data presented in this study are available on request from the corresponding author.

**Acknowledgments:** The authors wish to express their thanks to Adam Hunt and Bridget Stewart from the Materials Processing Institute, Middlesbrough, UK for providing access to experimental facilities.

**Conflicts of Interest:** The authors declare no conflict of interest.

## References

1. Huang, X.H.; Liao, L.; Zheng, K.; Hu, H.H.; Wang, F.M.; Zhang, Z.T. Effect of  $B_2O_3$  addition on viscosity of mould powder slag containing low silica content. *Ironmak. Steelmak.* **2014**, *41*, 67–74. [[CrossRef](#)]
2. Zhao, H.; Wang, W.; Zhou, L.; Lu, B.; Kang, Y.B. Effects of MnO on crystallisation, melting, and heat transfer of CaO- $Al_2O_3$  based mold flux used for high Al-TRIP steel casting. *Metall. Mater. Trans. B* **2014**, *45*, 1510–1519. [[CrossRef](#)]
3. Shi, C.B.; Seo, M.D.; Cho, J.W.; Ki, S.H. Crystallisation characteristics of CaO- $Al_2O_3$  based mould flux and their effects on in-mold performance during high-aluminium TRIP steels continuous casting. *Metall. Mater. Trans. B* **2014**, *45*, 1081–1097. [[CrossRef](#)]
4. Cho, J.W.; Blazek, K.; Frazee, M.; Yin, H.; Park, J.H.; Moon, S.W. Assessment of CaO- $Al_2O_3$  based mold flux system for high aluminium TRIP casting. *ISIJ Int.* **2013**, *53*, 62–70. [[CrossRef](#)]
5. Fu, X.J.; Wen, G.H.; Tang, P.; Liu, Q.; Zhou, Z.Y. Effects of CaO/ $Al_2O_3$  ratio on crystallisation behaviour of CaO- $Al_2O_3$  based mould fluxes for high Al TRIP steel. *Ironmak. Steelmak.* **2014**, *41*, 341–342. [[CrossRef](#)]
6. Blazek, K.; Yin, H.; Skoczylas, G.; McClymonds, M.; Frazee, M. Development and evaluation of lime-alumina based mold powders for casting high aluminium TRIP steel grades. *Iron Steel Technol.* **2011**, *8*, 232–249.
7. Jiang, B.; Wang, W.; Sohn, I.; Wei, J.; Zhou, L.; Lu, B. A kinetic study of the effect of  $ZrO_2$  and CaO/ $Al_2O_3$  ratios on the crystallisation behaviour of a CaO- $Al_2O_3$ -based slag system. *Metall. Mater. Trans. B* **2014**, *45*, 1057–1067. [[CrossRef](#)]
8. Lu, B.; Chen, K.; Wang, W.; Jiang, B. Effects of  $Li_2O$  and  $Na_2O$  on crystallisation behaviour of lime-alumina based mold flux for Casting High-Al Steels. *Metall. Mater. Trans. B* **2014**, *45*, 1496–1509. [[CrossRef](#)]
9. Yan, W.; Chen, W.; Yang, Y.; Lippold, C.; McLean, A. Effect of CaO/ $Al_2O_3$  ratio on viscosity and crystallisation behaviour of mould flux for high Al non-magnetic steel. *Ironmak. Steelmak.* **2015**, *42*, 698–704. [[CrossRef](#)]
10. Seyrek, M.; Thackray, R. Investigation on Viscosity of CaO- $Al_2O_3$  Based Mould Fluxes for the Continuous Casting of High-Al Steels. *Mater. Proc.* **2021**, *3*, 13. [[CrossRef](#)]
11. Mills, K.C.; Courtney, L.; Fox, A.B.; Harris, B. The use of thermal analysis in the determination of the crystalline fraction of slag films. *Thermochim. Acta* **2002**, *391*, 175–184. [[CrossRef](#)]
12. DIFFRAC. *EVA User Manual*; Bruker AXS GmbH: Karlsruhe, Germany, 2013.
13. Dey, A.; Riaz, S. Viscosity measurement of mould fluxes using inclined plane test and development of mathematical model. *Ironmak. Steelmak.* **2013**, *39*, 391–397. [[CrossRef](#)]
14. Xiao, D.; Wang, W.; Lu, B. Effects of  $B_2O_3$  and BaO on the crystallisation behaviour of CaO- $Al_2O_3$  based mould flux for casting high-Al steels. *Metall. Mater. Trans. B* **2015**, *46*, 873–881. [[CrossRef](#)]
15. Lu, B.; Wang, W.; Li, J.; Zhao, H.; Huang, D. Effect of basicity and  $B_2O_3$  on the crystallisation and heat transfer behaviours of low fluorine mold flux for casting medium carbon steels. *Metall. Mater. Trans. B* **2013**, *44*, 365–376. [[CrossRef](#)]
16. Gao, J.; Wen, G.; Sun, Q.; Tang, P.; Liu, Q. The influence of  $Na_2O$  on the solidification and crystallisation behaviour of CaO- $SiO_2$ - $Al_2O_3$  based mould flux. *Metall. Mater. Trans. B* **2015**, *46*, 1850–1859. [[CrossRef](#)]
17. Wang, H.; Tang, P.; Wen, G.H. Effect of  $Na_2O$  on crystallisation behaviour and heat transfer of high Al steel mould fluxes. *Ironmak. Steelmak.* **2011**, *38*, 369–373. [[CrossRef](#)]
18. Mills, K.C. Structure and properties of slags used in the continuous casting of steel: Part 2 Specialist mould powders. *ISIJ Int.* **2016**, *56*, 14–23. [[CrossRef](#)]
19. Li, Z.; Thackray, R.; Mills, K.C. A test to determine crystallinity of mould fluxes. In *VII International Conference on Molten Slags Fluxes and Salts*; The South African Institute of Mining and Metallurgy: Johannesburg, South Africa, 2004.
20. Thombre, D.B. Estimation of glass-forming ability and glass stability of Lithium-Borosilicate glasses. *Int. J. Innov. Res. Sci. Eng. Technol.* **2016**, *2*, 124–132.
21. Turnbull, D. Under what conditions can a glass be formed? *Contemp. Phys.* **1969**, *10*, 473–488. [[CrossRef](#)]
22. Mills, K.C.; Carl-Ake, D. *The Casting Powders Book*, 1st ed.; Springer: Cham, Switzerland, 2017; p. 318.
23. Zanutto, E.D.; Coutinho, F.A.B. How many non-crystalline solids can be made from all the elements of the periodic table? *J. Non-Cryst. Solids* **2004**, *1*, 285–288. [[CrossRef](#)]
24. Sharda, S.; Sharma, P.; Sharma, V. A study of thermal stability and crystallisation kinetics of SbSeGe glassy alloys. In *ICMAEM-2017*; IOP Publishing: Bristol, UK, 2017.
25. Inoue, A.; Shen, B.; Takeuchi, A. Fabrication, properties and applications of bulk glassy alloys in late transition metal-based systems. *Mater. Sci. Eng. A* **2006**, *441*, 18–25. [[CrossRef](#)]
26. Inoue, A.; Zhang, T.; Masumoto, T. Glass-forming ability of alloys. *J. Non-Cryst. Solids* **1993**, *156–158*, 473–480. [[CrossRef](#)]
27. Hruby, A. Evaluation of glass-forming tendency by means of DTA. *Czechoslov. J. Phys. B* **1972**, *22*, 1187–1193. [[CrossRef](#)]
28. Yu, X.; Wen, G.H.; Tang, P.; Wang, H. Investigation on viscosity of mould fluxes during continuous casting of aluminium containing TRIP steel. *Ironmak. Steelmak.* **2013**, *36*, 623–630. [[CrossRef](#)]
29. Qi, J.; Liu, C.; Jiang, M. Properties investigation of CaO- $Al_2O_3$ - $SiO_2$ - $Li_2O$ - $B_2O_3$ - $Ce_2O_3$  mould flux with different  $w(CaO)/w(Al_2O_3)$  for heat-resistant steel continuous casting. *Can. Metall. Q.* **2017**, *56*, 212–220. [[CrossRef](#)]
30. McMillan, P.F.; Petuskey, W.T.; Cote, B.; Massiot, D.; Landron, C.; Coutures, J.P. A structural investigation of CaO- $Al_2O_3$  glasses via 27Al MAS-NMR. *J. Non-Cryst. Solids* **1996**, *195*, 261–271. [[CrossRef](#)]
31. Poe, B.T.; McMillan, P.F.; Cote, B.; Massiot, D.; Coutures, J.P. Structure and dynamics in calcium aluminate liquids: High-temperature 27Al NMR and Raman spectroscopy. *J. Am. Ceram. Soc.* **1994**, *77*, 1832–1838. [[CrossRef](#)]

32. Zhang, Z.; Wen, G.; Tang, P.; Sridhar, S. The influence of  $\text{Al}_2\text{O}_3/\text{SiO}_2$  ratio on the viscosity of mould fluxes. *ISIJ Int.* **2008**, *48*, 739–746. [[CrossRef](#)]
33. Yan, W.; McLean, A.; Yang, Y.; Chen, W.; Barati, M. Evaluation of mould flux for continuous casting of high-aluminium steel. In Proceedings of the 10th International Conference on Molten Slags, Fluxes and Salts (MOLTEN16), Seattle, WA, USA, 22–25 May 2016.
34. Kim, G.H.; Sohn, I. Role of  $\text{B}_2\text{O}_3$  on the viscosity and structure in the  $\text{CaO-Al}_2\text{O}_3\text{-Na}_2\text{O}$ -based system. *Metall. Mater. Trans. B* **2014**, *45*, 86–95. [[CrossRef](#)]
35. Fox, A.B.; Mills, K.C.; Lever, D.; Bezerra, C.; Valadares, C.; Unamuno, I.; Laraudogoitia, J.J.; Gisby, J. Development of fluoride-free fluxes for billet casting. *ISIJ Int.* **2005**, *45*, 1051–1058. [[CrossRef](#)]
36. Rudnitzki, J.; Shepherd, R.; Balichev, E.; Karrasch, S.; Krüger, F. Investigation of  $\text{Al}_2\text{O}_3$  pick-up in mould slag during continuous casting of Al containing steels. *Eur. Contin. Cast. Conf.* **2014**, *23*, 26.
37. Kim, M.S.; Lee, S.W.; Cho, J.W.; Park, M.S.; Lee, H.G.; Kang, Y.B. A reaction between high Mn-high Al steel and  $\text{CaO-SiO}_2$ -type molten mould flux: Part I. Composition evolution in molten mould flux. *Metall. Mater. Trans. B* **2013**, *44*, 299–308. [[CrossRef](#)]

**Disclaimer/Publisher’s Note:** The statements, opinions and data contained in all publications are solely those of the individual author(s) and contributor(s) and not of MDPI and/or the editor(s). MDPI and/or the editor(s) disclaim responsibility for any injury to people or property resulting from any ideas, methods, instructions or products referred to in the content.